Geophys. J. Int. (2010) **181,** 185–197 doi: 10.1111/j.1365-246X.2010.04525.x

Drop-down formation of deep basins along the Dead Sea and other strike-slip fault systems

Zvi Ben-Avraham,[1] Vladimir Lyakhovsky[2] and Gerald Schubert[3]

[1] *Department of Geophysics and Planetary Sciences, Tel-Aviv University, Tel-Aviv* 69978*, Israel*
[2] *The Geological Survey of Israel, Jerusalem* 95501*, Israel. E-mail: vladi@geos.gsi.gov.il*
[3] *Department of Earth and Space Sciences and Institute of Geophysics and Planetary Physics, University of California, Los Angeles,* CA 90095-1567*, USA*

Accepted 2010 January 16. Received 2009 December 8; in original form 2009 July 8

SUMMARY

We address the mechanism of sedimentary basin formation along strike-slip fault systems with 3-D numerical simulations based on a continuum damage rheology model. The formation of these basins is usually explained by a pull-apart mechanism that predicts a rhomb-shaped basin geometry bounded by two longitudinal strike-slip faults and two transverse listric faults. Significant ductile deformation of the lower crust and upper mantle associated with basin growth requires normal or elevated heat flux. The Dead Sea continental transform is associated with some of the larger and unusually deep basins, among which the southern Dead Sea is the deepest. The heat flow in the Dead Sea basin is anomalously low and it is associated with deep seismicity. Moreover, the basin is bounded by deep transverse normal faults rather than the listric faults required by the pull-apart model. Hence, the formation of the basin cannot be explained by the existing pull-apart model. Ben-Avraham and Schubert proposed an alternative conceptual model for the formation of the deepest basin at the southern Dead Sea. They suggested that an isolated block of lithosphere has dropped into the mantle. We simulate the formation of this and other deep basins along the Dead Sea fault and demonstrate that the 'drop down' mechanism of the Dead Sea basin formation suggested by Ben-Avraham & Schubert is possible. Density heterogeneities formed in the crust or upper mantle during a previous stage of regional magmatism, drop into the upper mantle when strike-slip faults are created and detach them from the surrounding lithosphere. The simulations indicate that the resulting basin is rhomb-shaped and that with time it grows by the addition of distinct segments to its edges. The proposed mechanism could account for the formation and evolution of large sedimentary basins along other strike-slip fault systems, such as the San Andreas fault and other continental transform faults.

Key words: Numerical solutions; Continental tectonics: strike-slip and transform; Sedimentary basin processes; Fractures and faults; Mechanics, theory, and modelling; Rheology: crust and lithosphere.

1 INTRODUCTION

Large shear faults are often associated with extensional sedimentary basins of various sizes usually referred to as pull-apart basins. The basins along the Dead Sea fault are among the deepest and largest in the world. Among these basins, the southern Dead Sea is extremely deep and is attracting much attention (Garfunkel & Ben-Avraham 1996; Al-Zoubi & ten Brink 2002; Ben-Avraham & Schubert 2006; ten Brink *et al.* 2006). The ratio of basin width to depth here and in other deep basins is occasionally less than one and sedimentary fill sometimes exceeds 10 km in thickness. The deepest segments are located within the southern Dead Sea basin and the southern Sea of Galilee basin (Fig. 1). Geological evidence suggests that these basins are the oldest structures, 17–18 Ma, associated with the Dead Sea transform (Garfunkel 1997). In areas where the deep basins occur, two strands of the Dead Sea fault overlap in an en-echelon pattern. This situation is quite rare along the Dead Sea fault. Normally most basins are bordered only on one side by a strand of the Dead Sea fault, leading to their asymmetry (Ben-Avraham 1985). This is also true for other continental transforms such as the San Andreas in California, El Pilar in Venezuela and Polichic in Guatemala (Ben-Avraham 1992). Where asymmetry occurs basins do not extend to great depth.

Depressions associated with extension along strike-slip fault systems where the sense of bending or en-echelon segment stepping coincides with the sense of the slip are usually interpreted as pull-apart basins (e.g. Aydin & Nur 1982; Christie-Blick & Biddle 1985). The pull-apart mechanism predicts that two sides of the basin are bounded by faults with primarily horizontal displacement, and the other two sides are bounded by listric faults. Local extension

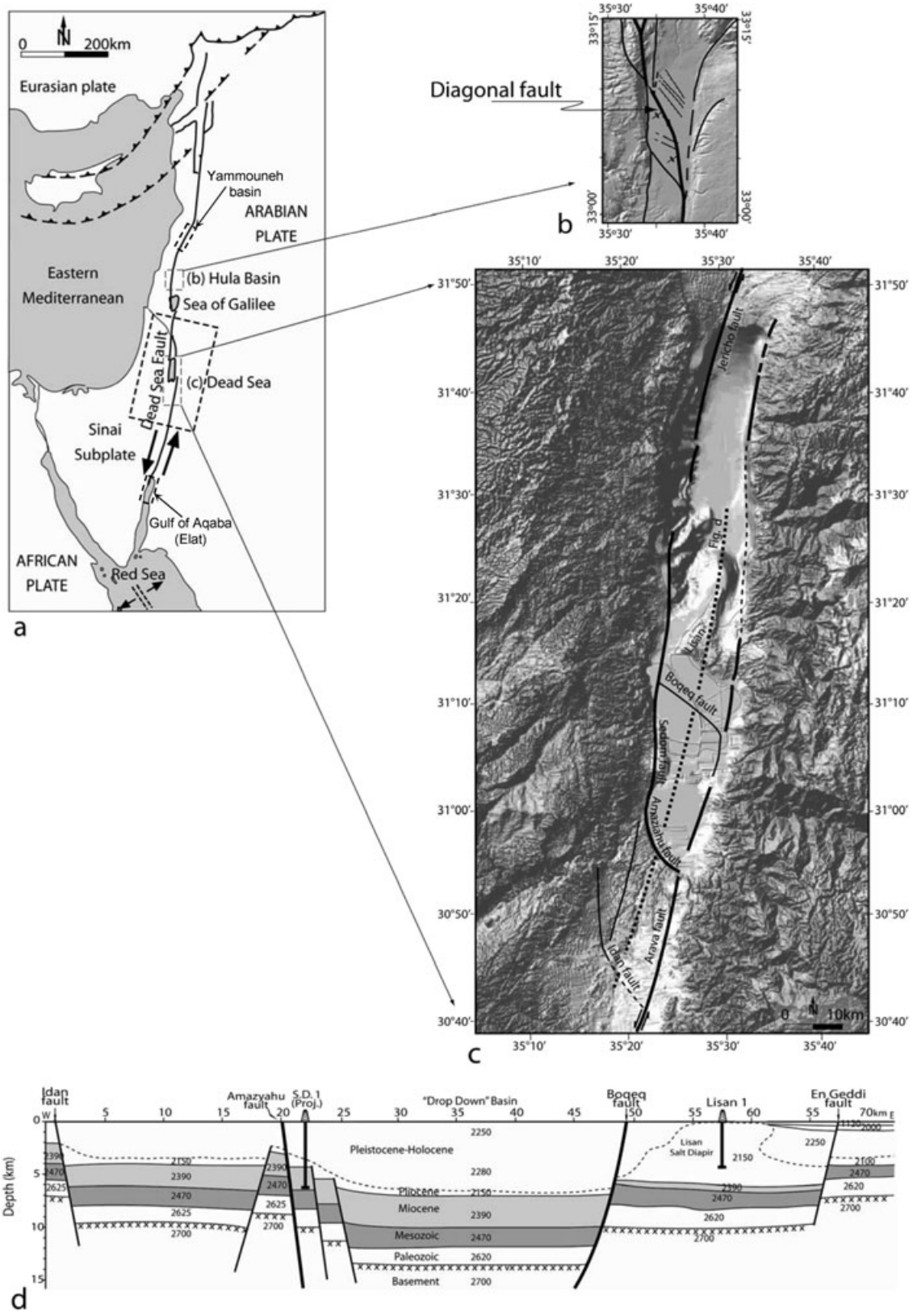

Figure 1. Location of the Dead Sea and other basins within the Dead Sea fault (a). DTM images of Hula (b) and Dead Sea (c) basins. Note that on the surface the Hula basin is rhomb-shaped; nevertheless, recent study (Schattner & Weinberger 2008) shows that the basin does not extend significantly at depth and the main strand of the Dead Sea fault in this area cuts the basin diagonally from southeast to northwest. In contrast, in the Dead Sea basin, which is divided into two subbasins, two main strands of the Dead Sea fault, the Jericho fault and the Arava fault border the basin on the west and on the east. The deep basin, at the northern part of the southern subbasin, is bounded by the Boqeq fault in the north, the Amazyahu fault in the south, the Sedom fault, an extension of the Jericho fault, in the west, and the Arava fault in the east. Surface location of the model is shown by the heavy dashed rectangle.

accommodated in the brittle upper crust is accompanied by significant ductile deformation of the lower crust and upper mantle. Recent studies (Sobolev *et al.* 2005; Petrunin & Sobolev 2006; Smit *et al.* 2008) suggest that formation of a deep pull-apart basin such as the Dead Sea basin requires a ductile lower crust corresponding to normal or high heat flow. However, the heat flow is anomalously low in the Dead Sea basin (Ben-Avraham *et al.* 1978; Eckstein & Simmons 1978; Shalev *et al.* 2007). The Dead Sea basin is also associated with deep seismicity (Aldersons *et al.* 2003; Shamir 2006) and is bounded by deep transverse normal faults in the southern part rather than the listric faults required by the pull-apart model (Ginzburg *et al.* 2007). Therefore the formation of the Dead Sea basin cannot be explained by existing pull-apart models.

Measurements of the geometric complexity of faults (Wesnousky 1988, 1994; Stirling *et al.* 1996) demonstrate that the density of step offsets in the examined fault traces decreases as a function of cumulative slip, showing an evolution with continuing deformation from a disordered network of linked fault segments to simpler dominant localized fault zones. Additional observations and modelling (Ben-Zion & Sammis 2003; Lyakhovsky & Ben-Zion 2009; Finzi *et al.* 2009) indicate progressive evolution of fault structures toward increasing localization and geometric simplicity. Numerical simulations of the long-term evolution of a large strike-slip fault zone initially produce a system of stepping en-echelon segments that evolves with continuing deformation to a through-going localized structure. Recent geodynamic models of restraining and releasing bends along strike-slip faults (Li & Liu 2007; Li *et al.* 2009) also demonstrate that such bends along strike-slip faults typically result in concentrations of strain energy that favour development of newer faults cutting across the fault bends. Marco (2007) has suggested that a localization of faulting in the Dead Sea fault takes place as long as there is no change in the stress field. He showed that faulting along the Dead Sea transform began in the early–middle Miocene over a wide zone of up to 50 km and later, by the end of the Miocene, became localized. An interesting example is the Hula Basin north of the Sea of Galilee (Fig. 1). While the surface expression is of a rhomb shaped basin, a recent study (Schattner & Weinberger 2008) showed that the basin is relatively shallow and the main strand of the Dead Sea fault in this area cuts the basin diagonally from southeast to northwest. Nemer *et al*. (2008) recently studied evolution of the Yammouneh sedimentary basin (see Fig. 1 for location) along the main active branch of the Dead Sea transform fault within the Lebanese restraining bend. Figs 2(a)–(c) (modified after Nemer *et al.* 2008) schematically represents the suggested tectonic evolution starting with a fault step-over (a), displacement is primarily accommodated by faults bounding the rhomb-shape basin according to the classical pull-apart mechanism (b). Subsequently, a younger fault develops within the basin and accommodates all strike-slip movement (c). Limited normal faulting along the margins of the basin may continue, but the original step-over faults are generally inactive. Ehrhardt *et al.* (2005) described a similar situation in the northern Gulf of Aqaba (Elat). The main strand of the Dead Sea fault (Fig. 2d) bounds the eastern margin of the basin to the south, cuts diagonally across the basin at the northern Gulf of Aqaba from SE to NW (Elat fault) and joins the strand of the Dead Sea fault to the north (Evrona fault).

How then were the deep basins along the Dead Sea fault and other shear zones formed when the tendency of the fault zone is to become smooth and localized? In spite of this tendency, the longitudinal faults bordering the deep basins remain almost at the same distance from each other during the evolution of the basins as also suggested by the pull-apart models of basin formation. However, in contrast with the pull-apart model, it was demonstrated in some cases that the transverse faults bordering the deep basins also remain equidistant during their evolution (Ben-Avraham & Schubert 2006; Ginzburg *et al.* 2007). It is also unclear how the length of a pull-apart basin and the thickness of its sediments are determined and how the associated extensional strain is distributed at depth beneath the basin. Geological arguments (Garfunkel & Ben-Avraham 1996) as well as gravity data (ten Brink *et al.* 1993) suggest that the deformation pattern beneath the Dead Sea basin may change significantly from upper crust to lower crust and to mantle lithosphere. In the case of the Dead Sea basin, it is not understood why the supposedly extended crust is apparently not accompanied by a significantly uplifted Moho (ten Brink *et al.* 2006).

Recently Ben-Avraham & Schubert (2006) proposed a conceptual model of a 'drop-down' mechanism for the formation of the Southern Dead Sea basin. According to their suggestion, propagating faults isolated a block of lithosphere that dropped into the mantle. However, a quantitative description of this process was not presented.

In this work, we address the origin and evolution of the deep basin along the Dead Sea fault by 3-D numerical simulations in a model with a seismogenic crust governed by a continuum damage rheology. The damage rheology approach has several advantages in reproducing brittle rock deformation compared to the classical rigid elastic-plastic model of a solid governed by Byerlee's law (e.g. Brace & Kohlstedt 1980). A realistic rheological model of the faulting process should include subcritical crack growth from the very early stages of loading, material degradation due to increasing crack concentration, macroscopic brittle failure, post failure deformation, and healing. Among different approaches accounting for gradual material degradation are Robinson's (1952) linear cumulative creep damage law, Hoff's (1953) ductile creep rupture theory, Kachanov's (1958, 1986) brittle rupture theory, Rabotnov's (1959, 1988) coupled damage creep theory and many modifications of these theories (e.g. Valanis 1990; Papa 1993; Hansen & Schreyer 1994; Kachanov 1994; Krajnovic 1996; Allix & Hild 2002; Newman & Phoenix 2001; Shcherbakov & Turcotte 2003; Turcotte *et al.* 2003). Several authors pointed out that damage rheology is the most appropriate continuum framework for analysing large deformation in the upper crust (e.g. Turcotte & Glasscoe 2004), and used this approach for simulating irreversible deformation in a brittle layer on the top of a convecting mantle (e.g. Auth *et al.* 2003; Bercovici 2003; Regenauer-Lieb & Yuen 2003). The thermodynamically based two-phase model for compaction and damage of Bercovici *et al*. (2001), Ricard & Bercovici (2003) and Bercovici & Ricard (2003) accounts for viscous rock deformation but leaves out elasticity. That model was successfully applied to study shear localization and plate boundary formation, but is not appropriate for analysis of brittle failures in the seismogenic zone where elastic deformation plays the dominant role. The rate- and state-dependent (RS) friction model (e.g. Dieterich 1979, 1981; Ruina 1983) provides a framework that can be used to simulate important aspects of fault evolution, including stable slip, nucleation of instabilities, rupture propagation, and healing. However, the RS formulation assumes that deformation at all stages occurs on well-defined frictional surfaces, and it does not provide a mechanism for understanding distributed deformation. In this study we use the viscoelastic scalar damage rheology model of Lyakhovsky *et al.* (1997) and Hamiel *et al*. (2004). The governing equations of the damage rheology model, numerical simulations of evolving fault zone structures in a 3-D lithospheric model and relevant references are summarized in Lyakhovsky & Ben-Zion (2009) and Finzi *et al*. (2009).

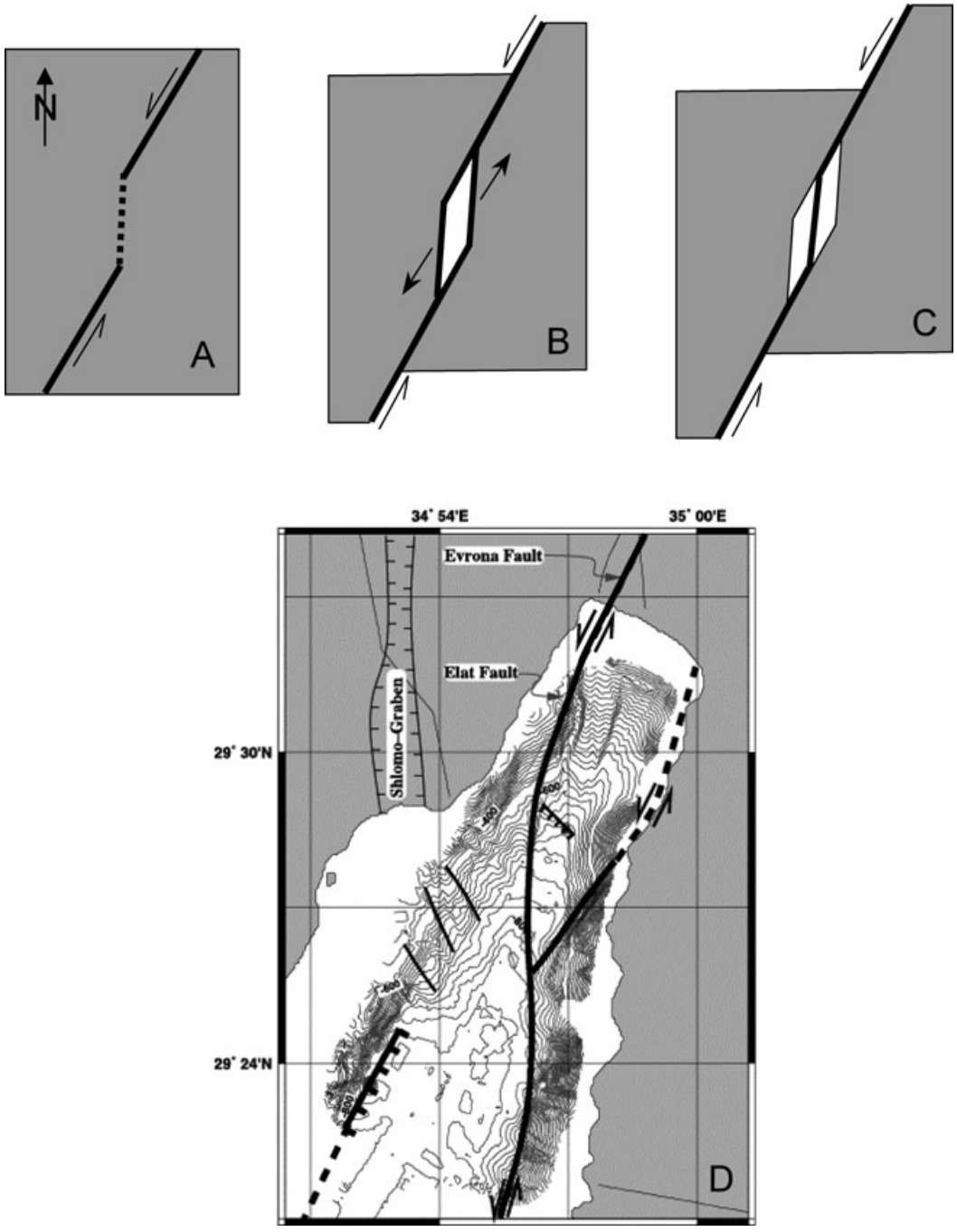

Figure 2. Yammouneh and northern Gulf of Aqaba (Elat) sedimentary basins (see Fig. 1 for location) and the diagonal faults cutting the basins. (a)–(c) Schematic representation of the Yammouneh basin tectonic evolution from the classical pull-apart basin to a formation of the younger fault within the basin which accommodates all the strike-slip movement (modified after Nemer *et al*. 2008). (d) Fault map deduced from the reflection seismic data (modified after Ehrhardt *et al*. 2005). The solid lines mark the observed fault system the dashed lines indicate the possible continuations of the faults.

The numerical modelling demonstrates that the 'drop-down' mechanism of the Dead Sea basin formation, suggested by Ben-Avraham & Schubert (2006) is possible. We propose here that dropping down of pre-existing heavy magmatic bodies into the mantle is the main mechanism driving the basin formation. Density heterogeneities, formed in the crust or upper mantle during previous phases of regional magmatic activity terminated well before the Dead Sea formation, dropped into the upper mantle only when strike-slip faults were created. Thus, the present model connects the processes that have led to the basin formation and the Dead Sea fault itself and provides an explanation of the main features of the basin.

2 DEAD SEA BASIN

The Dead Sea fault has several unique characteristics. The mean value of the corrected heat flow data for the northern part of the Dead Sea basin is 38 mW m^{-2} (Ben-Avraham *et al.* 1978). This value is comparable with nearby continental average values of 42 mW m^{-2} obtained by measurements in abandoned wells west of the lake (Eckstein & Simmons 1978). Recent re-evaluation of

the heat flow data (Shalev *et al.* 2007) confirmed these low values. Another characteristic of a large part of the Dead Sea fault is its anomalous deep seismicity, extending almost to the mantle (Aldersons *et al.* 2003; Shamir 2006). Sixty per cent of well-constrained microearthquakes ($M_L \leq 3.2$) in the Dead Sea basin for the period 1984–1997 nucleated at depths of 20–32 km and more than 40 per cent occurred below the depth of peak seismicity situated at 20 km. The deep seismic activity is consistent with a low heat flow of 40 mW m^{-2}, and suggests that the lower crust might be cold and brittle. This situation is quite different from that of the San Andreas fault, where the majority of the seismic activity takes place in the upper crust above ∼15 km depth (e.g. Magistrale 2002; Rolandone *et al.* 2004). The slip rate for the San Andreas Fault is several times higher than for the Dead Sea fault. Hence, one might expect a deeper seismogenic zone in California. The difference between the heat fluxes, 60–80 mW m^{-2} in California (e.g., Blackwell & Steele 1992) and ∼40 mW m^{-2} in the Dead Sea, could possibly be responsible for the anomalous deep seismicity along the Dead Sea fault. With this heat regime, a mathematical model by Petrunin & Sobolev (2008) suggests that the deep pull-apart basin might be created only if the pre-existing major faults are essentially frictionless. The formation of the diagonal fault cutting the basin is not allowed by the modelling procedure adopted by these authors (Sobolev *et al.* 2005; Petrunin & Sobolev 2006, 2008).

Seismic refraction and gravity data indicate that the northern part of the southern Dead Sea basin is unusually deep, with about 14 km of sedimentary fill (Ginzburg & Ben-Avraham 1997; Ben-Avraham & Schubert 2006). Geophysical data suggest that the deep basin is probably bordered on all sides by vertical faults that cut deep into basement (Ginzburg *et al.* 2007). A similar situation exists in the southern Sea of Galilee basin (Reznikov *et al.* 2004).

Magmatic events are recorded in the late Proterozoic Arabian–Nubian Shield of Sinai, southern Israel, Jordan, northern Saudi Arabia, and the Eastern Desert of Egypt over the past 900 Myr (Stein & Ben-Avraham 2007). After the end of the Pan African Orogeny magmatic activity in the entire region occurred in several pulses in Early Mesozoic, Early Cretaceous, Late Cretaceous and Neogene to recent times (Garfunkel 1989; Gvirtzman & Garfunkel 1997, 1998). These events have led to heterogeneous crust in the Middle East with great variability in the lithology expressed by several regional magnetic anomalies. The largest anomaly in the vicinity of the Dead Sea basin is the Hebron magnetic anomaly, which was interpreted (Rybakov *et al.* 1995) as a large basic magma body of unknown age penetrating the Permo-Triassic sediments. The age of the latest magmatic activity around the Dead Sea basin is more than a hundred million years (e.g. Garfunkel 1989). Magma intrusion of this age placed in the lower crust (20–30 km depth) beneath the Dead Sea should be completely cooled prior to the Dead Sea basin formation. This is consistent with evidence discussed above that supports a low surface heat flow and relatively cold lower crust.

Interpretation of gravity and topography data (ten Brink *et al.* 1990) leaves room for several versions of the Moho offset across the Dead Sea transform including a deep heavy intrusion in the lower crust (20–30 km depth) beneath the Dead Sea. Analyses of the morphology and structure of the crust and lithosphere using gravity, topography and seismic data reveal that at present the Dead Sea fault is not compensated isostatically and deep heterogeneities are expected (Segev *et al.* 2006). Wdowinski & Zilberman (1996, 1997) noted large-scale topographic and structural asymmetry across the Dead Sea fault, which resembles an uplifted shoulder on the eastern side and a wide arch on the west. Wdowinski & Zilberman (1996) used a kinematic isostatically supported half-graben model to calculate average uplifted structures mostly attributed to unloading of the surface.

Numerical simulation (Ben-Avraham & Lyakhovsky 1992; Lyakhovsky *et al.* 1994) of the propagation of faulting activity along the entire Dead Sea fault took into consideration both the opening of the Red Sea in the south and the collision processes in the Taurus Mountains in the north. This mathematical model of the evolution of the Dead Sea fault suggests that it was created as a result of the propagation of two fracture zones at its northern and southern ends towards each other. The simulation outlined only the general trend of the Dead Sea fault. Ben-Avraham & Schubert (2006) suggested that the tips of the two propagating rifts met in the area of the southern subbasin of the Dead Sea.

3 MODEL FORMULATION

We study the proposed mechanism of deep basin formation due to dropping down of a pre-existing heavy magma body into the mantle by simulating the evolving seismicity and fault pattern in a 3-D numerical model with the sizes 250 × 150 km and 70 km depth. The model consists of three different layers (Fig. 3): weak sediments (3 km thick); crystalline crust up to Moho (30 km depth); upper mantle. A relatively small (∼10 km radius), but heavy spherical magma body is embedded at Moho depth. We combine damage rheology reproducing brittle rock deformation in the seismogenic zone with power-law laboratory-based ductile rheology for the lower crust and upper mantle. The total strain tensor ε^t_{ij} in each layer is written as the sum of three strain components associated with different deformation mechanisms

$$\varepsilon^t_{ij} = \varepsilon_{ij} + \varepsilon^i_{ij} + \varepsilon^d_{ij}, \tag{1}$$

where the elastic strain $\varepsilon_{ij}$and the damage-related inelastic strain ε^i_{ij} are calculated using the damage rheology approach briefly discussed below. ε^d_{ij} represents ductile strain governed by Newtonian viscosity in the sedimentary layer and by the power-law relation between the shear stress τ and the strain rate $\dot{\varepsilon}$ (e.g. Weertman 1978) in the lower crust and upper mantle:

$$\dot{\varepsilon} = A\tau^n \exp\left(-\frac{Q + PV^*}{R_g T}\right). \tag{2}$$

The parameters A and n are empirical constants, Q is activation energy, V^* is activation volume, P is pressure, T is temperature, and R_g is the gas constant. A, n and Q values are presented in Table 1 together with other material parameters of the damage rheology model. For relatively low pressures corresponding to depths less than 100 km, the PV* term in (2) is negligible. For the lower crust we use the material constants appropriate for diabase rocks (Carter & Tsenn 1987), wet olivine for the upper mantle (Hirth & Kohlstedt 2003); and eclogite parameters for the inclusion (Jin *et al.* 2001). Material parameters controlling the ductile strain component are presented in Table 1.

The simulations incorporate a depth-dependent temperature distribution, corresponding to a pre-defined surface heat flow that is kept constant during the simulation. Following Turcotte & Schubert (2002), we assume that the heat production due to radioactive elements decreases exponentially with depth and use the depth-dependent temperature $T(z)$

$$T(z) = T_0 + \frac{qz}{k} + \frac{\rho_c H h^2}{k}\left(1 - \mathrm{e}^{-z/h}\right), \tag{3}$$

where $T_0 = 300$ K is the surface temperature, $k = 3.35$ Wm^{-1}K^{-1} is the coefficient of thermal conductivity, $q = 40$ mW m^{-2} is the

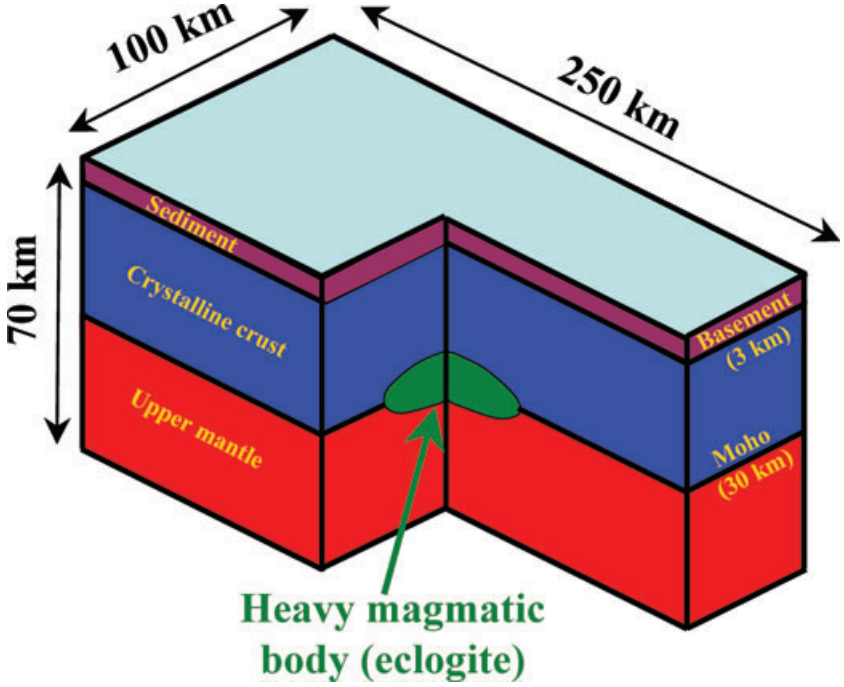

Figure 3. A schematic diagram of the 3-D lithospheric structure used in the numerical simulations.

heat flow, H is the surface radiogenic heat production and h is the length scale of its exponential decay. For the radiogenic component of the continental heat flow we take $\rho_c H = 3.7 \times 10^{-3}$ mW m^{-3} and $h = 10$ km.

The governing equations of the damage rheology model, their thermodynamic basis and experimental verification are presented in Lyakhovsky *et al.* (1997) and Hamiel *et al*. (2004). Discussion of the model and numerical results demonstrating evolving fault zone structures have been recently presented by Lyakhovsky & Ben-Zion (2009), Finzi *et al*. (2009) and references therein. Here we only briefly discuss the main features of the damage rheology adopted for the present study and sensitivity of the results to the model parameters. The model provides a quantitative treatment of the macroscopic effects of evolving distributed cracking with local density represented by an intensive damage state variable varying from zero for intact rock to one at total failure. The damage model accounts for three general aspects of brittle rock deformation including (1) mechanical response of a solid with an existing crack density, (2) kinetic changes associated with the evolution of the crack density and (3) macroscopic brittle instability (seismic event). This physical framework allows calculation of the simultaneous evolution of damage and its localization into narrow highly damaged zones (faults), earthquakes and associated deformation fields. Synthetic earthquake catalogues generated during the model runs enable analysis of coupled evolution of faults and seismicity pattern. The material parameters for each layer are listed in Table 1. The elastic moduli of the damage-free rocks are estimated from typical values of the rock density and seismic wave velocities widely accepted in the geophysical literature. In a thermomechanics framework of the damage rheology, the condition for the onset of damage accumulation is derived from the basic thermodynamic balance equations (e.g. Lyakhovsky *et al.* 1997) and is formulated in terms of strains. The strain invariants ratio, $I_1/\sqrt{I_2}$ ($I_1 = \varepsilon_{kk}$ and $I_2 = \varepsilon_{ij}\varepsilon_{ij}$ are two invariants of the elastic strain tensor ε_{ij}), controlling the transition from healing to damage accumulation (Lyakhovsky *et al.* 1997) is connected to the value of the internal friction angle of Byerlee's law (Byerlee 1978). The critical strain invariants ratio, $I_1/\sqrt{I_2} \sim -0.8$, is estimated using the internal friction angle of intact rocks and is well constrained. The kinetics of the damage accumulation (C_d value) is associated with the duration of the sample loading from the onset of acoustic emission till its macroscopic failure in the rock mechanics laboratory experiment. The laboratory-constrained rate of damage accumulation is important for understanding the damage accumulation process leading to failure, but it has a minor effect on the geometrical properties of the new-created fault zones and earthquake statistics in regional-scale models (e.g. Finzi *et al.* 2009; Lyakhovsky & Ben-Zion 2009). The recovery of elastic moduli and material strengthening is associated with healing of microcracks and is favoured by high confining pressure, low shear stress and high temperature. Motivated by the observed logarithmic increase of the static coefficient of friction (e.g. Dieterich 1978, 1979), Lyakhovsky *et al.* (1997) used an exponential damage-dependent function with coefficients C_1, C_2 for the kinetics of healing. The rate of the damage (α) decrease under 3-D compactive strain (ε) is

$$\frac{\mathrm{d}\alpha}{\mathrm{d}t} = -C_1 \exp\left(\frac{\alpha}{C_2}\right)\varepsilon^2. \tag{4}$$

The damage model with exponential healing (4) reproduces the main observed features of rate- and state-dependent friction and some constraints for the coefficients C_1, C_2 might be obtained by comparing model calculations with laboratory frictional data. However, these estimations are not well resolved and leave a relatively wide range for their possible values. Some field-based estimates of the healing parameters are given in (Finzi *et al.* 2009). Previous study demonstrated that the efficiency of the material healing controlled by the C_1, C_2 values significantly affects the evolution of the geometrical complexity of the fault zone (Lyakhovsky & Ben-Zion 2009) and statistics of the simulated earthquakes (Ben-Zion *et al.* 1999). The process of fault zone localization and reduction of geometrical complexities including development of the

Table 1. Material properties.

Material unit	Density[a] ($kg\ m^{-3}$)	Seismic wave velocities[a] ($km\ s^{-1}$)		Elastic moduli for damage–free material[b] (GPa)		Strain invariant ratio at the onset of damage[c]	Damage-rate parameters		Seismic coupling[f] χ (%)	Ductile flow parameters[g]		
		Vp	*Vs*	λ_0	μ_0		C_d[d] (s^{-1})	C_1[e] (s^{-1})	C_2[e]	A ($Pa^{-n}\ s^{-1}$)	n	Q ($kJ\ mol^{-1}$)
Sedimentary layer	2400	4.5	2.7	14	18	–	–	–	–	1×10^{-22}	1	–
Crust	2800	6.3	3.8	30	40	−0.8	5	0.05	3×10^3	6.3×10^{-20}	3.05	276
Upper mantle	3300	8.0	4.6	70	70	−0.8	5	0.05	3×10^3	1.9×10^{-15}	3.0	420
Inclusion	3500	8.3	4.8	80	80	−0.8	5	0.05	3×10^3	7.9×10^{-18}	3.4	480

[a]Geophysical literature.
[b]Calculated according to the density and seismic wave velocity (a) using linear elasticity.
[c]Calculated using internal friction (Byerlee law) and Poisson ratio (e.g. Lyakhovsky *et al.* 1997).
[d]Estimated using the time interval from the onset of acoustic emission to the total sample failure in the rock mechanics laboratory experiment (Lyakhovsky *et al.* 1997; Hamiel *et al.* 2004 and others).
[e]Parameters controlling the rate of material recovery (healing); see Finzi *et al.* (2009) for discussion.
[f]Seismic coupling or the ratio between seismic and aseismic deformation is constrained from analysis of the palaeoseismicity and decay in the aftershock sequences.
[g]Carter & Tsenn (1987), Hirth & Kohlstedt (2003), and Jin *et al.* (2001).

diagonal fault cutting the pre-existing rhomb-shape sedimentary basin (Lyakhovsky & Ben-Zion 2009) is more efficient in more 'viscous' lithosphere, with higher background temperature and slower healing. Disordered complex structures are typical for colder lithosphere and less effective healing. However, in this case also the pre-existing rhomb-shape sedimentary basin is not a stable geological structure and is cut by an oblique fault zone after a time period corresponding to several earthquake cycles (Lyakhovsky & Ben-Zion 2009).

Comparisons between theoretical predictions and observed deformation and acoustic emission from laboratory experiments in granites and sandstones led Hamiel *et al.* (2004) to incorporate a gradual accumulation of a damage-related irreversible deformation, ε^i_{ij}, which starts to accumulate with the onset of material weakening. The rate of this inelastic strain accumulation is assumed to be proportional to the rate of damage increase. Ben-Zion & Lyakhovsky (2006) connected the rate of irreversible strain accumulation with partitioning between seismic and aseismic deformation in the seismogenic zone, a well recognized mode of deformation on various segments of active faults (e.g. Liu *et al.* 2007). They showed that the fraction χ of elastic strain released seismically, referred to as the seismic coupling coefficient, could be estimated from analyses of aftershock sequences. Following this approach and using analytical 1-D results corresponding to uniform deformation, Yang & Ben-Zion (2009) provided estimates of the relative χ-values in different regions of southern California. A direct estimate of the relative fraction of seismic deformation that characterizes a given fault system requires a comparison between the seismic slip and the geodetically observed deformation of the region. Along the Dead Sea Transform, the seismically estimated slip rate based on historical earthquakes accounts for only $\chi = 0.3$ of the total geologically estimated rate (Garfunkel 1981), and the 20th century seismicity accounts for only $\chi = 0.1$ of the geological slip (Salamon *et al.* 1996). This indicates that either a strong earthquake is overdue or that the missing slip is aseismic. Creep along the DST was reported by Finzi (2005) based on aseismic slip detected by InSAR measurements of surface deformation at a specific fault step-over zone along the Arava segment (Southern DST). For the period of 1995–2000, Finzi (2005) suggested that approximately 0.3–0.5 of the total slip along the Arava segment was released aseismically. Accounting for this uncertainty, for the seismogenic crust and intrusion we used $\chi = 0.5$ and 0.3 for the upper mantle. Together with the efficiency of the material healing and the heat regime, the seismic coupling significantly affects the rate of the fault zone localization, but the overall tendency of the fault zone evolution remains the same (e.g. Lyakhovsky & Ben-Zion 2009).

The numerical simulations were done using the Fast Lagrangian Analysis of Continua (FLAC) algorithm (Cundall & Board 1988; Cundall 1989; Poliakov *et al.* 1993; Ilchev & Lyakhovsky 2001). The volume is divided into tetrahedral elements of variable size that increase gradually from about 1 km in the seismogenic zone to about 5 km in the ductile region. The boundary conditions (Fig. 4), corresponding approximately to the southern Dead Sea transform region, consist of left-lateral plate motion with a rate of about 5 mm yr^{-1}. The boundary forces applied to the vertical edges of the model are proportional to the slip-deficit between the prescribed constant far field plate motion and displacement of the boundary nodes through virtual springs. These boundary conditions account for the evolution of elastic properties and plastic strain in the model region (Lyakhovsky & Ben-Zion 2009). The applied boundary conditions include displacement discontinuities in the regions where the red lines in Fig. 4, corresponding to pre-existing strike-slip faults

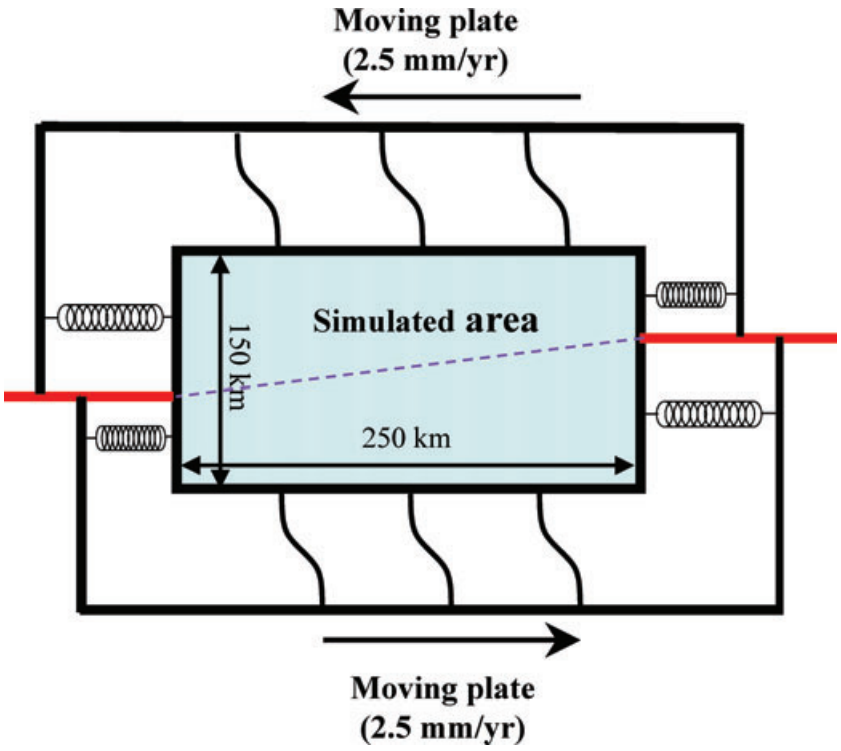

Figure 4. A schematic diagram illustrating the generalized boundary conditions corresponding to a constant plate motion far from the simulated model region. The red lines correspond to pre-existing strike-slip faults outside the simulated volume.

outside the simulated domain, cross the edges of the simulated volume. They are located according to the geometry of the Dead Sea transform outside the simulated area. The top of the model is free and the bottom boundary is fixed in the vertical direction and free to slip horizontally. The simulation starts with a stress distribution corresponding to a lithostatic pressure without any differential stress and low randomly distributed damage with damage parameter in the range 0–0.2.

4 NUMERICAL RESULTS AND DISCUSSION

In the first series of model runs (not shown here) we simulated the 'static' conditions without any tectonic loading associated with the motion of the Arabian plate. In the case of the relatively small intrusion assumed in this study, some elastic flexure compensates the buoyancy forces. The size of the intrusion and density difference are not big enough to initiate any observable dropping down of the intrusion or faulting around it. This is opposite to the delamination and detachment mechanism of the drip model (e.g. Lustrino 2005) of lower crustal and lithospheric mantle recycling. It has been proposed that under conditions of normal or elevated heat flux and large intrusion size, as in the case of delamination of the deep batholithic crust beneath the Sierra Nevada, California (Ducea & Saleeby 1996, 1998; Saleeby & Foster 2004; Zandt *et al*. 2004), buoyancy forces are large enough to guarantee convective removal of eclogite-rich mantle lithosphere (Molnar & Jones 2004).

Ongoing loading associated with the motion of the Arabian Plate and leading to the nucleation and development of the Dead Sea fault, causes stress amplification around the inclusion indicated by dashed circle (Fig. 5). Progressive steps every ∼250 000 yr. Panels (a)–(d) show the evolution of material damage at 10 km depth during ∼1 Ma of simulation. With time, the edges of the two propagating fault segments from north and south approach the area where the intrusion is located (Fig. 5a). At the next stage, new faults nucleate around the heavy body and detach it from the surrounding lithosphere (Fig. 5b). With time, new oblique segments cut the entire basin and are also formed north and south of the initial basin (Figs5c and d). The simulated rhomb-shaped basin progressively extends to the north and south by formation of new segments resembling previously discussed possible scenarios (ten-Brink & Ben-Avraham 1989; Lazar *et al.* 2006) of the Dead Sea basin formation. The created fault geometry mimics the pull-apart rhomb-shaped structure, but the mechanism of the basin formation is very different. One of the most important results of the model presented here is the development of the basin by the addition of distinct segments. After the formation of a segment, it deepens with time.

The heavy body detached from the surrounding lithosphere is not isostatically compensated; it starts sinking and pulls down the crustal block above it. This is expressed in the negative topography (Fig. 6) and gradual formation of the sedimentary basin. Initially, the isometric shape of the basin (Fig. 6a) reflects the spherical shape of the sinking heavy body. With formation of new fault segments the basin geometry (Figs 6b–d) is mostly controlled by the rhomb-shaped fault structure and becomes elongated. Detachment of the heavy body leads to the isostatic rebound of the flexure produced by the intrusion and some uplift of the E-W shoulders as discussed in the Wdowinski & Zilberman (1996, 1997) kinematic model. Continuous downward motion of the heavy body may lead to some additional uplift of the E–W shoulders. The schematic directions of motion together with the geometry of zones where large strain is accumulated are shown on the E–W profile (Fig. 7). The simulated subsidence rate of about 0.5 mm yr^{-1} is about ten times less than the slip rate along the Dead Sea fault. With these rates, ∼10 km of subsidence is expected during the period of up to 20 Ma when

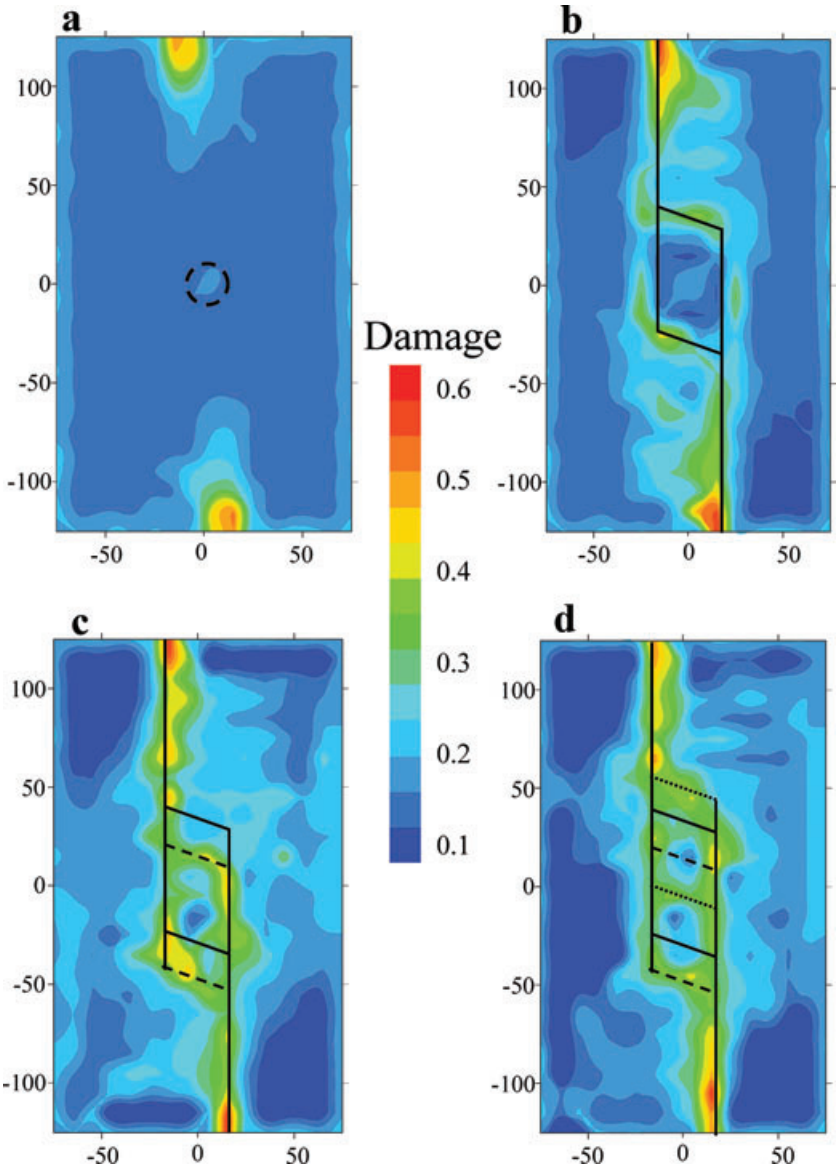

Figure 5. Progressive steps (a–d) in the evolution of material damage at 10 km depth in the simulated volume (see Fig. 1 for location). At the initial stage (a) two segments propagate in northern and southern directions from the model edges. Then a basin with rhomb-shaped geometry and transverse faults bordering the basin on the north and south are formed (b, heavy lines). At the next stage (c), an additional segment extending the basin to the south and another segment cutting the northern part of the basin are formed (dash lines). Heavy lines show the location of the segments formed at the previous stage (b). At a later stage (d), the northern and central segments are formed (dotted lines) in addition to those formed at stage c (dash lines) and stage b (heavy lines).

∼100 km of horizontal displacement was accumulated. Fig. 7 also shows the simulated distribution of seismicity with depth according to a synthetic catalogue of seismic events generated during the model run. Relatively cold lower crust leads to significant brittle deformation and seismicity even in the lower crust at depths below 25 km. The simulated depths of earthquakes are in agreement with observations of seismicity along the Dead Sea fault.

The total simulated slip along the fault zone is prescribed by the plate motion, while the derived seismicity pattern and evolving fault geometry depend on the inclusion size, rock strength, and material properties. The sensitivity of evolving geometrical and material properties of fault zones to the regional heat flow values and parameters of the damage rheology model was recently discussed by Lyakhovsky & Ben-Zion (2009). They connected the rate of the geometrical regularization process with the effective 'brittleness' of the model region. Following their study, complex fault geometry is expected in the model with cold and brittle lithosphere. However, even in the 'very brittle' lithosphere, complex geometrical structures have a clear tendency to localization in a homogeneously layered model or a model with a pre-existing sedimentary basin. In contrast to the Lyakhovsky & Ben-Zion (2009) results, in the model discussed here, the geometrical regularization process is not realized and new fault segments associated with dropping down of the intrusion are formed (Fig. 5). Instead of localization of deformation in a narrow zone obliquely cutting the sedimentary basin, geometrical complexity of the fault structure is gradually increased. The whole lithospheric block beneath the basin is sinking and most of the deformation is localized at its periphery (Fig. 7).

In southern California the Salton Trough may have been formed in a similar way, when the cracks associated with the opening of the Gulf of California propagated northward and met the San Andreas fault where it bends westward (Ben-Avraham and Schubert 2006).

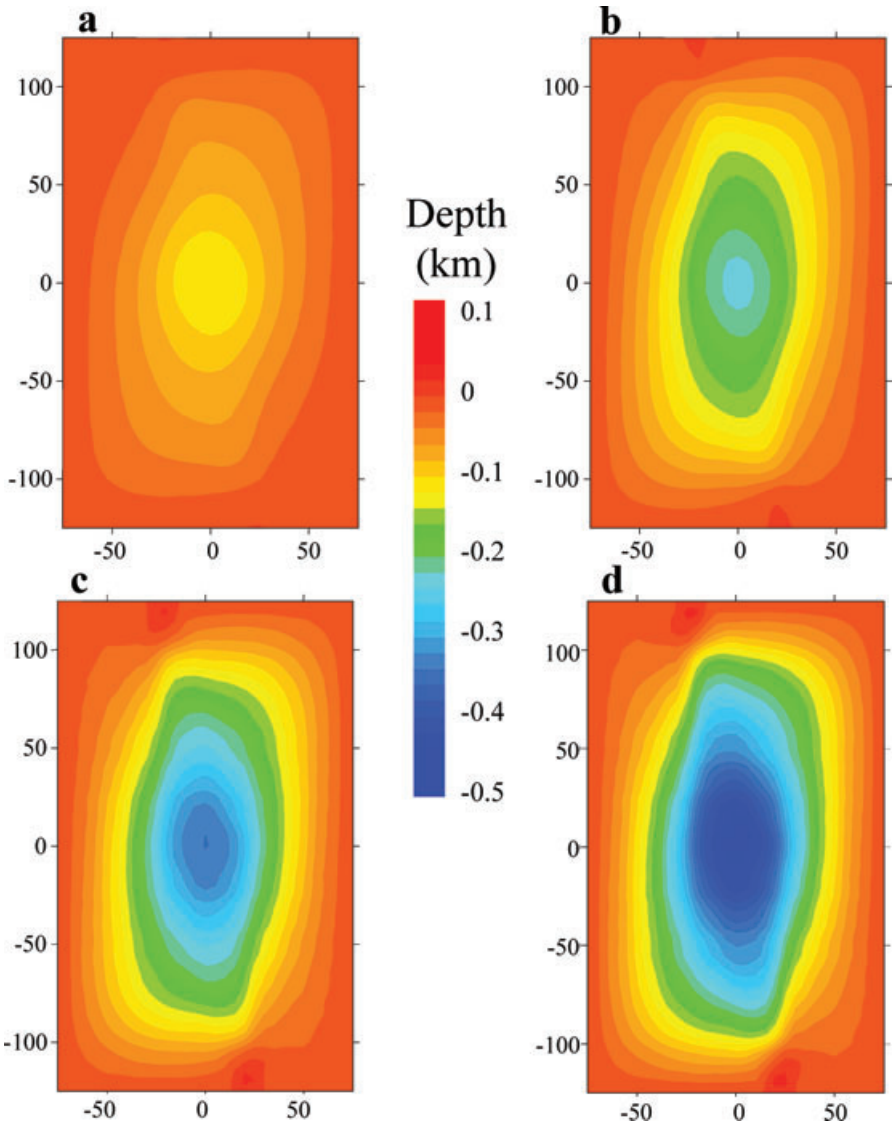

Figure 6. Progressive steps in the topographic evolution. Note the change of the basin from isometric shape to asymmetric and elongated in N–S direction. The initial shape of the basin is controlled by the spherical shape of the heavy inclusion, while at the later stages, interaction between ongoing strike- slip motion with the sinking block leads to a rhomb-shaped geometry.

This is the deepest basin along the entire San Andreas fault system, including the Gulf of California. It is possible that here also a heavy magmatic body in the lower crust was detached and dropped down when the two fault system met.

One of the most important model parameters is the size of the intrusion. A large and heavy magmatic intrusion starts sinking before the tectonic load is applied, while a very small intrusion produces negligible stress perturbation and a fault zone obliquely cutting the basin is formed. The suggested mechanism of the sedimentary basin formation requires a relatively small (∼10 km radius) intrusion. The intrusion size mostly controls the width of the sedimentary basin, while its weight, together with parameters controlling the kinetics of the damage evolution, define the rate of subsidence. The rate of gradual elongation of the sedimentary basin by formation of new fault segments is controlled by the rate of loading (plate motion) and parameters of the damage rheology model. Most of the rheological parameters, except those controlling the material recovery, are reasonably well constrained. The uncertainty in the rate of material healing mostly affects the number-magnitude distribution of the simulated earthquakes and the geometrical complexity of the obtained structures, but it has a minor effect on the general tendency of the basin evolution in the presented numerical model.

5 CONCLUSIONS

We investigate the origin and evolution of deep basins along the Dead Sea fault and propose that dropping down of pre-existing heavy magmatic bodies into the mantle is the main mechanism driving their formation. Density heterogeneities, formed in the crust or upper mantle during previous stages of regional magmatism, dropped into the upper mantle when strike-slip faults were created. Numerical simulations indicate that the resulting basin is rhomb-shaped and grows by the addition of distinct segments to its edges. Results of the modelling (Figs 5–7) suggest that the deepest part of the Dead Sea basin was formed first and later on the basin grew larger by extending to the north and south, a situation which is

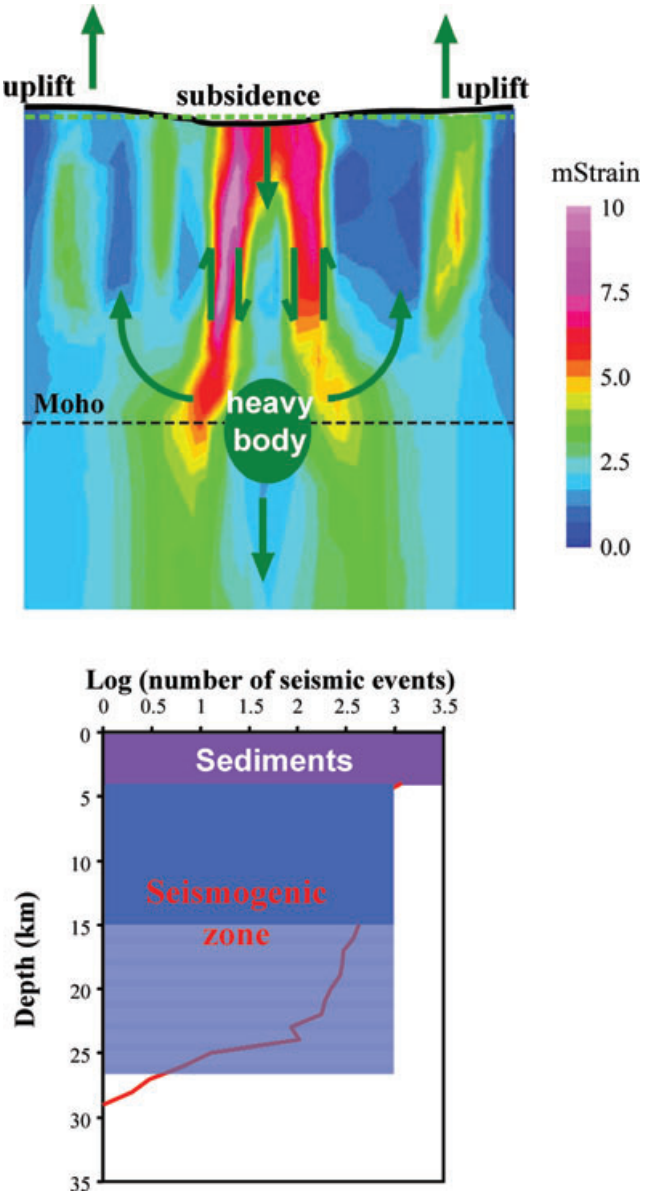

Figure 7. (A) Cumulative strain along E–W cross-section schematically demonstrating dropping down of the pre-existing spherical heavy magmatic body into the mantle. The colour represents accumulated strain (slip) on two faults bounding the heavy block (two sides of the block). (B) Seismicity distribution with depth. Simulated seismic activity extends up to more than 25 km depth in relatively cold lower crust.

probably also true for the southern Sea of Galilee in the north and the central Gulf of Aqaba, at the southern end of the Dead Sea fault. The proposed mechanism accounts for the observed heat flow and deep seismicity in the Dead Sea. We further argue that the mechanism proposed here is probably responsible for the formation of large and deep strike-slip basins along other continental transform faults, such as the San Andreas Fault.

ACKNOWLEDGMENTS

We thank the editor Y. Ricard and an anonymous referee for constructive reviews. V. Lyakhovsky acknowledges support from the Israel Science Foundation (grant ISF 753/08).

REFERENCES

Aldersons, F., Ben-Avraham, Z., Hofstetter, A., Kissling, E. & Al-Yazjeen, T., 2003. Lower-crustal strength under the Dead Sea basin from local earthquake data and rheological modeling, *Earth planet. Sci. Lett.,* **214,** 129–142.

Allix, O. & Hild, F., 2002. *Continuum Damage Mechanics of Materials and Structures,* Elsevier, Oxford, 396 pp.

Al-Zoubi, A. & ten-Brink, U., 2002. Lower crustal flow in small continental Basins: an example from the Dead Sea Basins, *Earth planet. Sci. Lett.,* **199,** 67–79.

Auth, C., Bercovici, D. & Christensen, U.R., 2003. Two-dimensional convection with self-lubricating, simple-damage rheology, *Geophys. J. Int.,* **154,** 783–800.

Aydin, A. & Nur, A., 1982. Evolution of pull-apart basins and their scale independence, *Tectonics,* **1,** 91–105.

Ben-Avraham, Z. & Lyakhovsky, V., 1992. Faulting processes along the Northern Dead Sea transform and the Levant margin, *Geology,* **20,** 1139–1142.

Ben-Avraham, Z. & Schubert, G., 2006. Deep "Drop Down" Basin in the Southern Dead Sea, *Earth planet. Sci. Lett.,* **251,** 254–263.

Ben-Avraham, Z., 1985. Structural framework of the Gulf of Elat (Aqaba)—northern Red Sea, *J. geophys. Res.,* **90,** 703–726.

Ben-Avraham, Z., 1992. Development of asymmetric basins along continental transform faults, *Tectonophys.,* **215,** 209–220.

Ben-Avraham, Z., Haenel R. & Villinger H., 1978. Heat flow through the Dead Sea rift, *Marine Geol.,* **28,** 253–269.

Ben-Zion, Y. & Lyakhovsky, V. 2006. Analysis of aftershocks in a lithospheric model with seismogenic zone governed by damage rheology, *Geophys. J. Int.,* **165,** 197–210.

Ben-Zion, Y. & Sammis, C., 2003. Characterization of Fault Zones, *Pure appl. Geophys.,* **160,** 677–715.

Ben-Zion, Y., Dahmen, K., Lyakhovsky, V., Ertas, D. & Agnon, A., 1999. Self-driven mode switching of earthquake activity on a fault system, *Earth planet. Sci. Lett.,* **172,** 11–21.

Bercovici, D. & Ricard, Y., 2003. Energetics of a two-phase model of lithospheric damage, shear localization and plate boundary formation, Geophys, *J. Int.,* **152,** 581–596.

Bercovici, D., 2003. The generation of plate tectonics from mantle convection, *Earth planet. Sci. Lett.,* **205,** 107–121.

Bercovici, D., Ricard, Y. & Schubert, G., 2001. A two-phase model for compaction and damage, part 1: general Theory, *J. geophys. Res.,* **106,** 8887–8906.

Blackwell, D. & Steele, J., 1992. Decade of North American geology geothermal map of North America, Geological Society of America, Boulder, CO, 1:5,000,000 map.

Brace, W.F. & Kohlstedt, D.L., 1980. Limits on lithospheric stress imposed by laboratory experiments, *J. geophys. Res.,* **85,** 6248–6252.

Byerlee, J.D., 1978. Friction of rocks, *Pure appl. Geophys.,* **116,** 615–626.

Carter, N.L. & Tsenn, M.C., 1987. Flow properties of continental lithosphere, *Tectonophysics,* **136,** 27–63.

Christie-Blick, N. & Biddle, K.T., 1985. Deformation and basin deformation along strike-slip faults, in *Strike-Slip Deformation, Basin Formation, and Sedimentation,* eds Biddle K.T. & Christie-Blick N., Special Publication **37**, pp. 1–34, Soc. Economic Paleontologists Mineralogists, Tulsa, Oklahoma.

Cundall, P.A. & Board, M., 1988. A microcomputer program for modeling large-strain plasticity problems, in *Numerical Methods in Geomechanics, Proceedings 6th International Conference Numerical Methods in Geomechanics, Innsbruck,* pp. 2101–2108, ed. Swoboda C., Balkema, Rotterdam.

Cundall, P.A., 1989. Numerical experiments on localization in frictional materials, *Ign. Arch.,* **59,** 148–159.

Dieterich, J.H., 1978. Time-dependent friction and the mechanics of stick-slip, *Pure appl. Geophys.,* **116,** 790–805.

Dieterich, J.H., 1979. Modeling of rock friction 1. Experimental results and constitutive equations, *J. geophys. Res.,* **84,** 2161–2168.

Dieterich, J.H., 1981. Constitutive properties of faults with simulated gouge, in *Mechanical behavior of Crustal Rocks,* eds Carter N.L., Friedman M., Logan J.M., Sterns D.W., *Am. Geophys. Union Monogr*. **24**, 103–120. Am. Geophys. Union, Washington, DC.

Ducea, M.N. & Saleeby, J.B., 1996. Buoyancy sources for a large, unrooted mountain range, the Sierra Nevada, California; evidence from xenolith thermobarometry, *J. geophys. Res.,* **101,** 8229–8244.

Ducea, M.N. & Saleeby, J.B. 1998. A case for delamination of the deep batholithic crust beneath the Sierra Nevada, California, *Int. Geol. Rev.,* **133,** 78–93.

Eckstein, Y. & Simmons, G., 1978, Measurements and interpretation of terrestrial heat flow in Israel, *Geothermics.,* **6,** 117–142.

Ehrhardt, A., Hubscher, C., Ben-Avraham, Z. & Gajewski, D., 2005. Seismic study of pull-apart induced sedimentation and deformation in the Northern Gulf of Aqaba (Elat), *Tectonophysics,* **396,** 59–79.

Finzi, Y., 2005. Current deformation in the southern Dead Sea Transform: radar interferometry measurements and their tectonic implications, *Geol. Survey Israel Report* GSI/24/04.

Finzi, Y., Lyakhovsky, V., Ben-Zion, Y. & Hearn, E.H., 2009. Structural properties and deformation patterns of evolving strike-slip faults: numerical simulation incorporating damage rheology, *Pure appl. Geophys.,* **166,** 1537–1573.

Garfunkel, Z. & Ben-Avraham, Z., 1996. The structure of the Dead Sea basin, *Tectonophysics,* **226,** 155–176.

Garfunkel, Z., 1981. Internal Structure of the Dead Sea leaky transform (rift) in relation to plate kinematics, *Tectonophysics,* **80,** 81–108.

Garfunkel, Z., 1989. Tectonic setting of Phanerozoic magmatism in Israel, *Isr. J. Earth Sci.,* **38,** 51–74.

Garfunkel, Z., 1997. The history and formation of the Dead Sea basin, in *The Dead Sea: The Lake and Its Settings,* Vol. **36**, pp. 36–56, eds Niemi T.M., Ben-Avraham Z. & Gat J., Oxford University Press, New York.

Ginzburg, A. & Ben-Avraham, Z., 1997. A seismic refraction study of the north basin of the Dead Sea, Israel, *Geophys. Res. Lett.,* **24,** 2063–2066.

Ginzburg, A., Reshef, M., Ben-Avraham, Z. & Schattner, U., 2007. The style of transverse faulting in the Dead Sea basin from seismic reflection data: the Amazyahu fault, *Israel J. Earth Sci.,* **55,** 129–139.

Gvirtzman, Z. & Garfunkel, Z., 1997. Vertical movements following intracontinental magmatism: an example from southern Israel, *J. geophys. Res.,* **102,** 2645–2658.

Gvirtzman, Z. & Garfunkel, Z., 1998. The transformation of southern Israel from a swell to a basin: stratigraphic and geodynamic implications for intracontinental tectonics, *Earth planet. Sci. Lett.,* **163,** 275–290.

Hamiel, Y., Liu, Y., Lyakhovsky, V., Ben-Zion, Y. & Lockner, D. 2004. A visco-elastic damage model with applications to stable and unstable fracturing, *J. geophys. Int.,* **159,** 1–11.

Hansen N. R., & Schreyer, H. L., 1994. A thermodynamically consistent framework for theories of elasticity coupled with damage, *Int. J. Solids Struct.,* **31,** 359–389.

Hirth, G. & Kohlstedt, D.L., 2003. Rheology of the upper mantle and the mantle wedge: a view from the experimentalists, in the subduction factory, *Geophys. Monogr*. **138**, pp. 83–105, ed. Eiler, J., AGU, Washington, DC.

Hoff, N.J., 1953. The necking and rupture of rods subjected to constant tensile loads, *J. appl. Mech.,* **20,** 105–108.

Ilchev A. & Lyakhovsky V., 2001. Practical aspects of the hybridization of the boundary integral method with damage rheology modeling for the assimilation of seismic data, in *Dynamic Rock Mass Response to Mining, Rockbursts and Seismicity in Mines–RaSiM5,* pp. 421–426, eds van Aswegen G., Durrheim R.J. & Ortlepp W.D., South African Institute of Mining and Metallurgy, Johannesburg, SA.

Jin, Z.M., Zhang, J., Green, H.W. II & Jin, S., 2001. Eclogite rheology: implications for subducted lithosphere, *Geology,* **29,** 667–670.

Kachanov, L.M., 1958. On the time to rupture under creep conditions, *Izv. Acad. Nauk SSSR,* **OTN 8,** 26–31 (in Russian).

Kachanov, L.M., 1986. *Introduction to Continuum Damage Mechanics,* Martinus Nijhoff Publishers, 135 p.

Kachanov, M., 1994. On the concept of damage in creep and in the brittle-elastic range, *Int. J. Damage Mech*., **3,** 329–337.

Krajcinovic, D., 1996. *Damage Mechanics,* Elsevier, Amsterdam.

Lazar, M., Ben-Avraham, Z. & Schattner, U., 2006. Formation of sequential basins along a strike-slip fault, geophysical observations from the Dead Sea basin, *Tectonophysics,* **421,** 53–69.

Li, Q. & Liu, M., 2007. Initiation of the San Jacinto fault and its interaction with the San Andreas fault: insights from geodynamic modeling, *Pure appl. Geophys.,* **164,** 1937–1945.

Li, Q., Liu, M. & Zhang, H., 2009. A 3-D viscoelastoplastic model for simulating long-term slip on non-planar faults, *Geophys. J. Int.,* **176,** 293–306.

Liu, Y., Rice J. R., & Larson, K. M., 2007. Seismicity variations associated with aseismic transients in Guerrero, Mexico, 1995–2006, *Earth planet. Sci. Lett.,* **262,** 493–504.

Lustrino, M., 2005. How the delamination and detachment of lower crust can influence basaltic magmatism, *Earth-Sci. Rev.,* **72,** 21–38.

Lyakhovsky, V. & Ben-Zion, Y., 2009. Evolving geometrical and material properties of fault zones in a damage rheology model, *Geochem. Geophys. Geosyst.,* **10,** Q11011, doi: 10.1029/2009GC002543.

Lyakhovsky, V., Ben-Avraham, Z. & Achmon, M., 1994. The origin of the Dead Sea rift, *Tectonophysics,* **240,** 29–43.

Lyakhovsky, V., Ben-Zion, Y. & Agnon, A., 1997. Distributed damage, faulting, and friction, *J. geophys. Res.,* **102,** 27,635–27,649.

Magistrale, H., 2002. Relative contributions of crustal temperature and composition to controlling the depths of earthquakes in southern California, *Geophys. Res. Lett.,* **29**(10), 1447.

Marco, S., 2007. Temporal variation in the geometry of a strike–slip fault zone: examples from the Dead Sea Transform, *Tectonophysics,* **445,** 186–199.

Molnar, P. & Jones, C.H., 2004. A test of laboratory based rheological parameters of olivine from an analysis of late Cenozoic convective removal of mantle lithosphere beneath the Sierra Nevada, California, USA, *Geolphys. J. Int.,* **156,** 555–564.

Nemer, T., Gomez, F., Al Haddad, S. & Tabet, C., 2008. Coseismic growth of sedimentary basins along the Yammouneh strike-slip fault (Lebanon), *Geophys. J. Int.,* **175,** 1023–1039.

Newman W.I. & Phoenix S.L., 2001. Time-dependent fiber bundles with local load sharing, *Phys. Rev. E.,* **63**(2), 021507, doi:10.1103/PhysRevE.63.021507.

Papa, E.A, 1993. Damage model for concrete subjected to fatigue loading, *Eur. J. Mech., A/Soids,* **12,** 429–440.

Petrunin, A.G. & Sobolev, S.V., 2006. What controls thickness of sediments and lithospheric deformation at a pull-apart basin? *Geology,* **34,** 389–392.

Petrunin, A.G. & Sobolev, S.V., 2008. Three-dimensional numerical models of the evolution of pull-apart basins, *Phys. Earth. planet. Inter.*, **171,** 387–399.

Poliakov, A., Cundall, P., Podladchikov, Y. & Lyakhovsky, V., 1993. An explicit inertial method for the simulation of viscoelastic flow: an evaluation of elastic effects on diapiric flow in two- and three-layers model, in *Proceedings of the NATO Advanced Study Institute on Dynamic Modeling and Flow in the Earth and Planets,* pp. 175–195, eds Runcorn K.E. & Stone D., Kluwer, Dordrecht.

Rabotnov, Y.N., 1959. A mechanism of a long time failure, in *Creep Problems in Structural Members,* pp. 5–7, USSR Academy of Sci. Publ., Moscow.

Rabotnov, Y.N., 1988. Mechanics of deformable solids, Moscow, *Science,* 712.

Regenauer-Lieb, K. & Yuen, D.A., 2003. Modeling shear zones in geological and planetary sciences: solid-and fluid-thermal—mechanical approaches, *Earth-Sci. Rev.,* **63,** 295–349.

Reznikov, M., Ben-Avraham, Z., Garfunkel, Z., Gvirtzman, H. & Rotstein, Y., 2004. Structural and stratigraphic framework of lake Kinneret, *Israel J. Earth Sci.,* **53,** 131–149.

Ricard, Y. & Bercovici, D., 2003. Two-phase damage theory and crustal rock failure: the theoretical ''void'' limit, and the prediction of experimental data, *Geophys. J. Int.,* **155,** 1057–1064.

Robinson, E.L., 1952. Effect of temperature variation on the long-term rupture strength of steels, *Trans. Am. Soc. Mech. Eng.,* **174,** 777–781.

Rolandone, F., Bürgmann, R. & Nadeau, R.M., 2004. The evolution of the seismic-aseismic transition during the earthquake cycle: constraints from

the time-dependent depth distribution of aftershocks, *Geophys. Res. Lett.,* **32**, doi:10.1029/2004GL21379.

Ruina, A.L., 1983. Slip instability and state variable friction laws, *J. geophys. Res.,* **88,** 10,359–10,370.

Rybakov, M., Fleisher, L. & Goldshmidt, V., 1995. A new look at the Hebron magnetic anomaly, *Isr. J. Earth-Sci.,* **44,** 41–49.

Salamon, A., Hofstetter, A., Garfunkel, Z. & Ron, H., 1996. Seismicity of the eastern Mediterranean region: perspective from the Sinai subplate, *Tectonophysics,* **263,** 293–305.

Saleeby J. & Foster, Z., 2004. Topographic response to mantle lithosphere removal in the southern Sierra Nevada region, California, *Geology,* **32,** 245–248.

Schattner, U. & Weinberger, R., 2008. A mid-Pleistocene deformation transition in the Hula basin, northern Israel: implications for the tectonic evolution of the Dead Sea Fault, *Geochem. Geophys. Geosyst.,* **9,** Q07009.

Segev, A., Rybakov, M., Lyakhovsky, V., Hofstetter, A., Tibor, G., Goldshmidt, V. & Ben Avraham, Z., 2006. The structure, isostasy and gravity field of the Levant continental margin and the southeast Mediterranean area, *Tectonophysics,* **425,** 137–157.

Shalev, E., Lyakhovsky, V. & Yechieli, Y., 2007. Is advective heat transport significant at the Dead Sea basin? *Geofluids,* **7,** 292–300.

Shamir, G., 2006. The active structure of the Dead Sea depression, in *New Frontiers in Dead Sea Paleoenvironmental Research,* Geological Society of America Special Paper 401, pp. 15–32, eds Enzel Y., Agnon A. & Stein, M, Geological Society of America, Inc., Boulder CO, doi:10.1130/2006.2401(02).

Shcherbakov R. & Turcotte D.L., 2003. Damage and self-similarity in fracture, *Theor. Appl. Fracture Mech.,* **39,** 245–258.

Smit, J., Brun, J.-P., Cloetingh, S. & Ben-Avraham, Z., 2008. Pull-apart basin formation and development in narrow transform zones with application to the Dead Sea Basin, *Tectonics,* **27,** TC6018.

Sobolev, S.V., Petrunin, A., Garfunkel, Z., Babeyko, A.Y., DESERT Group, 2005. Thermomechanical model of the Dead Sea transform, *Earth planet. Sci. Lett.,* **238,** 78–95.

Stein M. & Ben-Avraham, Z., 2007. Mechanism of continental crust growth, in *Treatise on Geophysics*, Vol. 9: Evolution of the Earth, pp. 171–195, eds Schubert, G. & Stevenson, D., Elsevier, Amsterdam.

Stirling, M.W., Wesnousky, S.G. & Shimazaki, K., 1996. Fault trace complexity, cumulative slip, and the shape of the magnitude-frequency distribution for strike-slip faults: a global survey, *Geophys. J. Int.,* **124,** 833–868.

ten Brink, U.S., Al-Zoubi, A.S., Flores, C.H., Rotstein, Y., Qabbani, I., Harder, S.H. & Kelle, G.R., 2006. Seismic imaging of deep low-velocity zone beneath the Dead Sea basin and transform fault: implications for strain localization and crustal rigidity, *Geophys. Res. Lett.,* **33,** L24314.

ten Brink, U.S., Ben-Avraham, Z., Bell, R.E., Hassouneh, M., Coleman, D.F., Andeasen, G., Tibor, G. & Coakley, B., 1993. Structure of the Dead Sea pull-apart basin from gravity analyses, *J. geophys. Res.*, **98,** 21,877–21,894.

ten Brink, U.S., Schoenberg, N., Kovach, R. & Ben Avraham, Z., 1990. Uplift and a possible Moho offset across the Dead Sea transform, *Tectonophysics,* **180,** 71–85.

ten-Brink, U.S. & Ben-Avraham, Z., 1989. The anatomy of a pull-apart basin: seismic reflection observations of the Dead Sea, *Tectonics,* **8,** 333–350.

Turcotte, D.L. & Glasscoe, M.T., 2004. A damage model for the continuum rheology of the upper continental crust, *Tectonophysics,* **383,** 71–80.

Turcotte, D.L. & Schubert, G., 2002. *Geodynamics,* 2nd edn, John Wiley & Sons, New York.

Turcotte, D.L., Newman, W.I., & Shcherbakov, R., 2003. Micro and macroscopic models of rock fracture, *Geophys. J. Int.,* **152,** 718–728.

Valanis, K.C., 1990. A theory of damage in brittle materials, *Eng. Fract. Mech.,* **36,** 403–416.

Wdowinski, S. & Zilberman, E. 1996. Kinematic modeling of large-scale structural asymmetry across the Dead Sea Rift, *Tectonophysics,* **266,** 187–201.

Wdowinski, S. & Zilberman, E. 1997. Systematic analyses of the large scale topography and structure across the Dead Sea Rift, *Tectonics,* **16,** 409–424.

Weertman, J., 1978. Creep laws for the mantle of the Earth. Philos, *Trans. R. Soc. Lond. A,* **288,** 9–26.

Wesnousky, S., 1988. Seismological and structural evolution of strike-slip faults, *Nature,* **335,** 340–342.

Wesnousky, S., 1994. The Gutenberg-Richter or characteristic earthquake distribution, which is it? *Bull. seism. Soc. Am.,* **84,** 1940–1959.

Yang, W. & Y. Ben-Zion, 2009. Observational analysis of correlations between aftershock productivities and regional conditions in the context of a damage rheology model, *Geophys. J. Int.,* **177,** 481–490.

Zandt, G., Gilbert, H., Owens, T.J., Ducea, M., Saleeby, J. & Jones, C.H., 2004. Active foundering of a continental arc root beneath the southern Sierra Nevada in California. *Nature,* **431,** 41–46.